Data center holistic demand response algorithm to smooth microgrid tie-line power fluctuation

Ting YANG

Yingjie ZHAO

Haibo PEN

Zhaoxia WANG
Singapore Management University, zxwang@smu.edu.sg

Data center holistic demand response algorithm to smooth microgrid tie-line power fluctuation

Ting Yang[a], Yingjie Zhao[a], Haibo Pen[a], Zhaoxia Wang[b]

[a] Key Laboratory of Smart Grid of Ministry of Education (Tianjin University), Tianjin 300072, China

[b] Institute of High Performance Computing, Agency for Science, Technology and Research, 138632, Singapore

Published in Applied Energy, 2018 December, 231, 277-287.
DOI: 10.1016/j.apenergy.2018.09.093

Abstract

With the rapid development of cloud computing, artificial intelligence technologies and big data applications, data centers have become widely deployed. High density IT equipment in data centers consumes a lot of electrical power, and makes data center a hungry monster of energy consumption. To solve this problem, renewable energy is increasingly integrated into data center power provisioning systems. Compared to the traditional power supply methods, renewable energy has its unique characteristics, such as intermittency and randomness. When renewable energy supplies power to the data center industrial park, this kind of power supply not only has negative effects on the normal operation of precision equipment, such as CPU/GPU chips and hard disk, in data center, but it would also impact the stability of the utility power grids operation. To solve this problem, this paper presents a novel tie-line power fluctuation smoothing algorithm with consideration of data center's holistic demand response. The contributions of this paper are: (1) overcoming the limitations of treating IT load as uncontrollable workload in the traditional demand response research, we design a data center resource scheduling model to realize IT load demand response controllability; (2) two novel mechanisms are proposed: (i) the server cluster workload scheduling method with time shift mechanism, and (ii) the data center UPS (Uninterruptible Power Supply) energy storage dynamic response mechanism. (3) Combining these two mechanisms as holistic demand response of data center, we present a tie-line power fluctuation smoothing algorithm to improve power supply reliability, which is beneficial to both the high density and precision IT equipment in the data center and the utility power grid. In the experiments, the results show that the new algorithm can effectively regulate the tie-line power fluctuations under different server cluster utilization ranges and scenarios of large-scale penetration of distributed renewable energy scenarios. The new algorithm is hence able to contribute beneficially to the reliability and stability of intelligent industrial park micro-grid and utility power grids.

Keywords: Controllable load, Data center, Holistic demand response, Tie-line power control

1 Introduction

With the rapid development of cloud computing, artificial intelligence technologies and the big data applications, Intelligent Park with data centers are increasing in number. There are often tens or hundreds of thousands of servers to bear complex computing tasks, which consume huge amounts of power. Four years before, in 2013,total energy consumption by data centers' computing equipment around the world is 0.5% of total global annual electricity consumption. By 2020, the percentage will double to 1% [1]. According to statistics, the Microsoft Quincy data center, located in Washington. DC, has a peak electricity consumption of up to 48MW, which is equivalent to the sum of 40,000 households electrical power consumption [2]. In another example, the US National Security Agency's giant data center located in Utah, the electric power consumption has reached an even higher peak of 70 MW [3]. High electricity and huge carbon emission pressure result in the suppliers having to reconsider the energy consumption of data centers. Renewable energy, such as wind or photovoltaic power, is used widely to realize sustainable development [4,5]. There are many studies on the optimal methods for maximizing renewable energy utilization, or minimizing the electricity expenses of data center [6,7].

However, unlike the traditional power supply, renewable energy has intermittency and randomness problems [8,9]. When such unstable power is supplied to data centers, it will cause power fluctuations in the tie-line between data centers and the electrical power grid. To data centers, a classical type of sensitive power load, the poor power quality has adverse effects on the precision equipment, such as CPU/GPU chips and hard disk. It also breaks the stability of the power grid operation [10]. This problem will become more serious with the increase of renewable energy penetration.

To the best of our knowledge, no research has been conducted on the issue of power quality with data center load in intelligent park micro-grid. In this paper, the intermittency and randomness of renewable energy and its adverse effects on data center are studied, and then a novel tie-line power fluctuation smoothing algorithm is presented.

The major contributions of this paper can be summarized as follows.

- We overcome the limitation of treating IT load as uncontrollable workload in the traditional demand response situation, and design a data center resource scheduling model to realize high density IT power load's demand response controllability.
- Two novel mechanisms, the server cluster workload scheduling method with time shift mechanism and data center UPS energy storage dynamic response mechanism are proposed in the paper. Combining these two mechanisms as holistic demand response of data center, a tie-line power fluctuation smoothing algorithm is presented to improve power supply reliability, which is beneficial to both the high precision IT equipment in the data center and the power grid.

The remainder of the paper is organized as follows: Section 2 briefly reviews related work in the field. In Section 3, the data center demand response model is established, and the tie-line power fluctuation smoothing algorithm is proposed in Section 4. Section 5 presents the experimental results of our algorithm under different power supply scenarios, and the efficiency of demand response control with different parameters are also evaluated. We conclude the paper in Section 6.

2. Background and related work

In recent years, there has been preliminary studies on the renewable energy applications in data centers [11], which can be sorted mainly into the following three categories. The first category is carrying out data center energy allocation planning. On the premise of meeting the demand of data centers' energy consumption, many studies make contributions to optimizing the different energy supply combination to minimize the data centers' operation overhead and carbon emission. With the increasing requirements on computing power, such as interplanetary exploration, cloud diagram analysis, seismic data mapping, and Bitcoin's mining, the huge energy engulf cannot be ignored. Independent researchers have estimated that just cryptocurrencies application alone is consuming around 500 megawatts annually [12,13]. The research reported in [14] focuses on data center backup power supply facility–UPS, and proposes the RE-UPS control strategy to realize the maximization of renewable energy utilization.

The second category involves research on the tasks scheduling mechanism in data centers to minimize the server cluster power consumption or maximize the utilization of renewable energy. The method reported in [15] proposes a maximizing data center revenue algorithm, which calculates the real-time renewable energy output and electricity price, and dynamically schedules tasks. The similar optimal function with minimizing electricity costs was studied in [16]. The research reported in [17] presents a power management scheme named iSwitch, which redistributes load migration events among different wind power supplies.

The third category of research is in analyzing the characteristics of different kinds of renewable energy, building power models, and then redistributing the renewable energy source to match computing workload. The research reported in [18] uses time series method to establish the photovoltaic power models, and in [19] machine learning method is used to establish the wind power forecasting models. Based on these power forecasting models, optimal scheduling strategies are implemented in data centers. Previous work [20] has proposed a method for optimizing workload performance and load following efficiency in DG-powered data centers using power demand shaping (PDS).

Besides theoretical research, some well-known IT companies are also investing in this direction and have gradually built new data centers partly or entirely powered by renewable energy with the latest research methods. For example, a 40 MW solar array is being built by Apple for its North Carolina data center [21]; Facebook built a solar-powered data center in Oregon, a 14 MW solar array was recently completed by McGraw-Hill for its data center [22]; 30 large scale fuel cells is also planned by eBay [23] which will provide 6 MW power to its data center; bio-fuel based gas turbine has recently been considered by HP [24] to be used in its Net-Zero data center; a new wind-powered data center has been built by Green House data in Wyoming [25].

From the review above, all previous work focused on maximizing the utilization of renewable energy sources or reducing the electricity cost of data center. However, what is more important than the total power consumption is the power supply quality. With the unpredictable and intermittent distributed generation, such as in solar-wind hybrid systems, when connecting renewable energy to data centers, power supply quality becomes a problem that is more severe than ever before. This paper focuses on this issue and proposes a novel demand response tie-line power fluctuation smoothing algorithm to solve this problem.

3. Modeling of data center demand response

3.1. The micro-grid model with renewable energy generations and data centers load

In recent years, renewable energy has gained tremendous interest as an alternative source of power for the IT industry. An intelligent industrial park can be regarded as a micro-grid consisting of a hierarchy of power supply/distribution elements, which includes electric power generation, power conversion, power utilization, etc. There are issues related to computing servers as sensitive electrical load, cooling and lighting equipment as necessary electrical load, UPS as backup power unit, and power supply unit from utility power grids and renewable sources. In the following, we will discuss the main issues in three aspects.

Utility Power Grids: Because the conventional power grids have a large amount of capacity inertia and high stability, it always acts as data centers' primary power source to satisfy the high power supplying requirements from precision IT equipment. But the high power consumption results in the large-scale date centers having to face two serious consequences. First, high monthly electricity bills are incurred during peak capacities demand and at times of high demands [26]. Hence, millions of dollars annually may be incurred by a large data center. Second, in many geographical locations, much of the current main grids are still fossil fuel dependent. Therefore, data centers are faced with legislative or public opinion pressure to find other options for carbon footprint reduction [27].

There is a complementary way to address these issues through smarter strategies of electricity sourcing: distributed generations (DG) with renewable energy are deployed on-site at the data center facility itself. This means the supply is no longer necessarily tied to or tied as little as possible to the brown source from the utility power grids.

***Distributed Generation*:** DG refers to using a number of possibly different types of small, modular electric generators near the point of use, which including green/renewable energy sources such as photovoltaic power (PV), wind power, bio-fuel based gas turbine, and so on [28]. With the maturity of DG technology, it increasingly becomes the favorite of the IT industry by virtue of its remarkable performance.

(1) Photovoltaic Power Characteristics: Photovoltaic power, being a clean energy technology, does not cause environmental pollution as in fossil-fuel-fired power generation or nuclear energy. Using photovoltaic panels, such as monocrystalline and polycrystalline silicon, solar energy is transformed into direct-current (DC) electricity to drive through the electrical load. However, photovoltaic generation is closely tied to certain weather and environmental conditions (e.g., solar irradiance, temperature, clouds or buildings' shade), and hence, can be highly time-varying.

The PV cells are connected in string and/or parallel to achieve the corresponding voltage and current. The current–voltage characteristics of a PV cell can be described by the operating equation below [29]:

$$I = I_{ph} - I_s\left[\exp\left(\frac{q(U+R_sI)}{Ak_sT}-1\right)\right]-\frac{U+R_sI}{R_{sh}} \tag{1}$$

where I_{ph} is the photocurrent, I_S is the saturation current, q is the electronic charge, A is the ideality factor, k_s is the Boltzmann's gas constant, T is the junction temperature (in kelvin), R_s is the series resistance, and R_{sh} is the shunt resistance. Eq. (1) presents the fact that the maximum output current I_{om} will change strongly non-linear with the different output voltage U_{om}. So the maximum output power $P_m = U_{om}I_{om}$ varies with the output voltage. Except for the solar irradiance, the environmental temperature also greatly affects the output voltage curve, as shown in Eq. (1) and the left figure in Fig. 1. For example, when the environmental temperature changes from $[-20\,°C, +40\,°C]$, the maximum power point of the voltage can drift up to 30% of the PV cell's open-circuit voltage. If there is no tracking and correction, the PV output power P_m will have losses exceeding 20% [30].

Partial shading conditions (PSCs) due to clouds, trees, or buildings is another problem: they weaken and vary the PV cell's output power, which result in multiple peaks on the *P-U* curve. String PV cells would give rise to hot spot effect when they are exposed to PSCs [30]. To avoid module-level hot spot, the output port of each PV cells is paired in parallel with a diode in the opposite direction. These bypass diodes change the PV array's output voltage U_{om} and current I_{om}, which results in the *P-U* curve of PV string exhibiting multiple local peaks in PSCs. In our previous work, we studied this problem in detail and proposed a

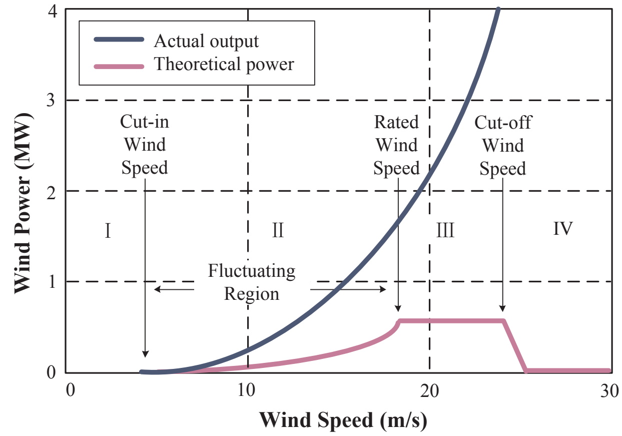

Fig. 2. Wind power output characteristics.

series of optimization algorithms to achieve maximum power point tracking (MPPT) [29,31]. The right figure of Fig. 1 presents our experiments on the output voltage waveform of the PV arrays under partially shaded condition.

(2) Wind Power Characteristics: Wind power derives electricity from the kinetic energy of air flow produced by wind turbines, which is also strongly related to environmental condition. Fig. 2 illustrates a typical GE wind turbine's output characteristics. The power curve shown is divided into four regions based on operating wind speeds [17].

In Region-I and IV (intermittent power outage period), due the wind speed being either too low or too high, wind power is intermittently unavailable. The "*cut-in speed*" refers to the minimum speed at which the rotor and blade starts to rotate, and the "*cut-off speed*" refers to the wind speed at which the turbine shuts down for the protection of the blade assembly. In Region-II (variable power generation period), the mechanical power delivered to the turbine generator is given by ($p = 0.5\rho Av^3C$) [32], where ρ is the air density, A is the swept area of the blades, v is the wind speed and C is the power coefficient factor. In Region-III (stable power generation period), the wind turbine operates at its designated rated power.

Even in Region-II, wind power also has the highest variability. M. Patel, et al. studied the variations in wind speed and presented it as the *Weibull* distribution [32]:

$$f(v) = \left(\frac{k}{c}\right)\cdot\left(\frac{v}{c}\right)^{k-1}\cdot e^{-\left(\frac{v}{c}\right)^{k}} \quad cut\text{-}in\ speed \leqslant v \leqslant cut\text{-}off\ speed \tag{2}$$

where k is the shape parameter, and c is the scale parameter. Based on statistics from most wind farm sites, it can be shown that the wind speed has the *Weibull* distribution with $k = 2$, which is specifically known as the *Rayleigh* distribution. As a result, in Region-II, the wind

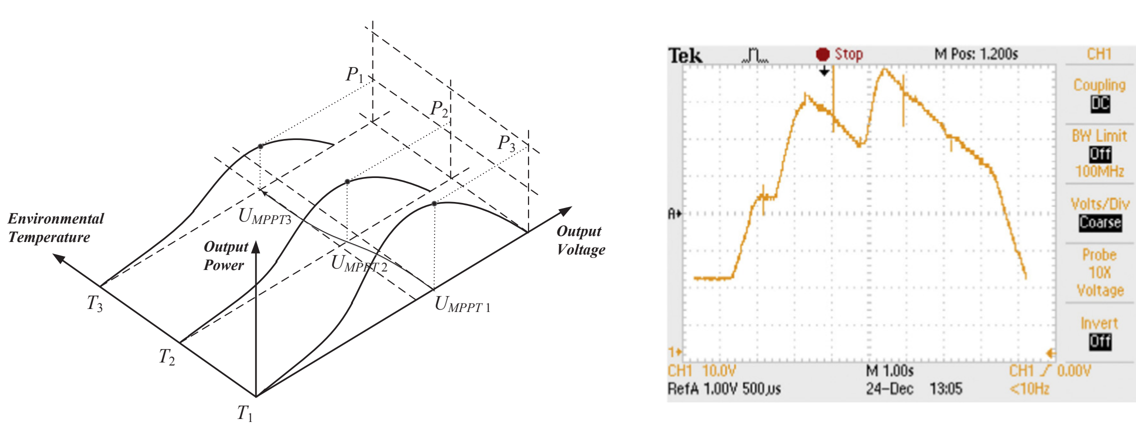

Fig. 1. Experimental output voltage waveform of the PV arrays under different environmental temperature and partially shaded condition.

turbine is more likely to incur time-varying wind speed. In conclusion, the wind turbine output is a steep curve due to the cubic relation between wind power and wind speed. In this case, similar to photovoltaic power characteristics, a small change of environmental factor such as the wind speed can lead to large wind generation fluctuation.

Data center Power Infrastructure: The data center consumed power can be broadly categorized into two parts: energy used by IT equipment and usage by infrastructure facilities. As the crucial part of data centers, server clusters' equipment (e.g., CPU, networks, hard disk, etc.) consumes the most power provided to data centers, which is roughly 46%. The other part is infrastructure facilities, including air conditioners or chiller equipment (power consumption 31%), UPS + lighting (12%), and auxiliary facilities (11%) [33].

The power consumption of servers is for computation tasks, and a lot of heat is generation from the chips. It is almost linearly related to the CPU utilization rate [34]. In Section 3.2, the power consumption model of a computing server will be presented.

Each air conditioner or chiller equipment removes the heat h_c from the computer chip by consuming power P_c. The performance of an air conditioner can be expressed as h_c divided by P_c and is called the coefficient of performance (COP) [35]. COP, which represents the performance of air conditioners, is a function of temperature set point, volumetric airflow rate, load, outside air temperature, and other factors.

Data center facilities are considered critical infrastructures, in which any risk of information flow interruption caused by loss of power supply that may occur during computation or network loss of function. Energy storage technologies can increase the infrastructure tolerance to utility power grid failures and perturbations, and to improve reliability/availability of the power distribution system. A typical example is that South Australia's government utilized the Tesla battery electrical storage technique and established a 100-megawatt battery storage system to guard against the repetition of earlier energy crises, such as the blackouts of 28th September 2016 and February 2017 [36]. In a data center, the energy storage technology is realized by UPS equipment, in which a great number of redundant battery groups provides power backup and allow data centers to intentionally under-provision the power delivery infrastructure [37]. When load power demand surge arises, one can temporarily release the UPS stored energy to avoid power budget violation. Moreover, energy storage devices also facilitate emerging renewable power integration in data centers. Therefore, in this paper, we present a UPS energy storage model and realize the use of UPS units as one of the tools to smoothen the variation over time of the power output of renewable energy generation, thus provide stable power for data center.

When renewable energy is accessed to support the use of green power resource to solve data center's huge energy consumption problem, the intelligent industrial park becomes a real micro-grid with various components including complete electric power generation, power distribution, AC/DC transformation, and different types of power utilization. There are issues related to brown energy (generated from fossil fuels), green energy (generated from renewable energy), UPS energy storage, computing servers as sensitive electrical load, and other energy exchange and support devices. The structure of this micro-grid system is shown in Fig. 3. The power balance equation of this type of micro-grid is shown as Eq. (3), and the meaning of the symbols in the equation is presented in Table 1.

$$\sum P_{supply} = \sum P_{consume} \Rightarrow P_{TL,i} + P_{UPS,i} + P_{RE,i} = P_{clusters,i} + P_{CL,i} \tag{3}$$

From Eq. (3), the intermittency and randomness of renewable energy $P_{RE,i}$ are the cause of the data center tie-line power fluctuations. With the increasing renewable energy penetration, the tie-line power fluctuation becomes much more serious. It has adverse effects on the precision IT equipment and UPS storage devices. Therefore, it is necessary to have an effective control algorithm to smooth the tie-line power fluctuation and improve the power quality.

3.2. The model of server cluster workload scheduling

In traditional demand response research, IT equipment, especially the high density integration of tens of thousands of server clusters and refrigeration equipment in the data center, becomes a hungry monster of energy consumption [27], and is typically considered to be an uncontrollable power load with full capacity running. With the development of Virtual Machine (VM) and Software Defined Network (SDN) techniques, more finely controlled workflows and traffic flows in data center have been realized [38]. We proposed a data center workload scheduling model to realize IT load demand response controllability.

Because there is a difference in the arrival time of tasks from the user's computing requests, the data center's power consumption is time variant. When a large quantity of computing tasks arrives at the data centers, the data center's power consumption increases; on the contrary, the power consumption decreases. Therefore, the data center's power load curve presents a huge difference between peaks and valleys. As shown in the energy consumption statistics of a small data center in Facebook [39], its power load peak-valley difference in half an hour can account for 80% of its peak value of power load, and the maximum instantaneous fluctuation reaches 87%. The wide application of virtual machines and tasks scheduling technologies results in the data center's power load being flexible and adjustable [40], which means that the server cluster's power load can be dynamically controlled by migrating a certain number of tasks to different time periods. Therefore, in summary, the computing and power load characteristics of cloud computing data center have the following properties [41]: high peak value, large peak-valley difference, and controllability, which means that the server cluster is well suited to participate in power demand response.

Based on the above analysis, this paper proposes a server cluster workload scheduling model with a time shift mechanism. As the core units of data centers, server clusters are processing a large quantity of required computing tasks at all times [42]. According to the response time required by different user requests, the computing tasks can be sorted into *delay-sensitive tasks* and *delay-tolerant tasks*. Delay-sensitive tasks should be processed immediately without any delay. On the other side, the delay-tolerant tasks are only required to be completed before one regulation deadline. Fig. 4 shows the difference between the two types of task.

In the model, the task is set to an integer, i.e. any task is the integral multiple of the basic task units. The processing time of one basic task units is ΔT_b. When a delay-sensitive task arrives at $T_{s,Arr}$, the completed time should be $T_{s,Deadline} = T_{s,Arr} + \Delta T_b$. When a delay-tolerant task arrives at $T_{t,Arr}$, and its tolerable delay time interval is ΔT_{max_dl}, it must begin to process the task before time $T_{t,start} = T_{t,Arr} + \Delta T_{max\_dl}$ and the tolerable completion deadline is:

$$T_{t,Deadline\_max} = T_{t,start} + \Delta T_b = (T_{t,Arr} + \Delta T_{max\_dl}) + \Delta T_b \tag{4}$$

In other words, a delay-tolerant task can be delayed processing at any time point in $[T_{t,Arr}, T_{t,start}]$ freely. This paper uses just the characteristic of delay-tolerant tasks to schedule this type of tasks and processes in different time units. This leads to the controllability of the data centers' computing workload and power consumption.

The power consumption of a computing server is linearly related to the CPU utilization [33], which can be defined as:

$$P_{server} = P_{server}^{chassis} + P_{server}^{unit} \cdot \eta \tag{5}$$

where $P_{server}^{chassis}$ is the basic power consumption to keep memory, disks, and I/O resources running, and holding at around two thirds of its peak-load consumption, $P_{server}^{unit} \cdot \eta$ represents the remaining one-third power consumption, which changes almost linearly with the increase of the CPU load. P_{server}^{unit} is unit power consumption. η is the server's resource utilization, which can be calculated by Eq. (7).

In a data center, all servers are assumed to be isomorphic. The

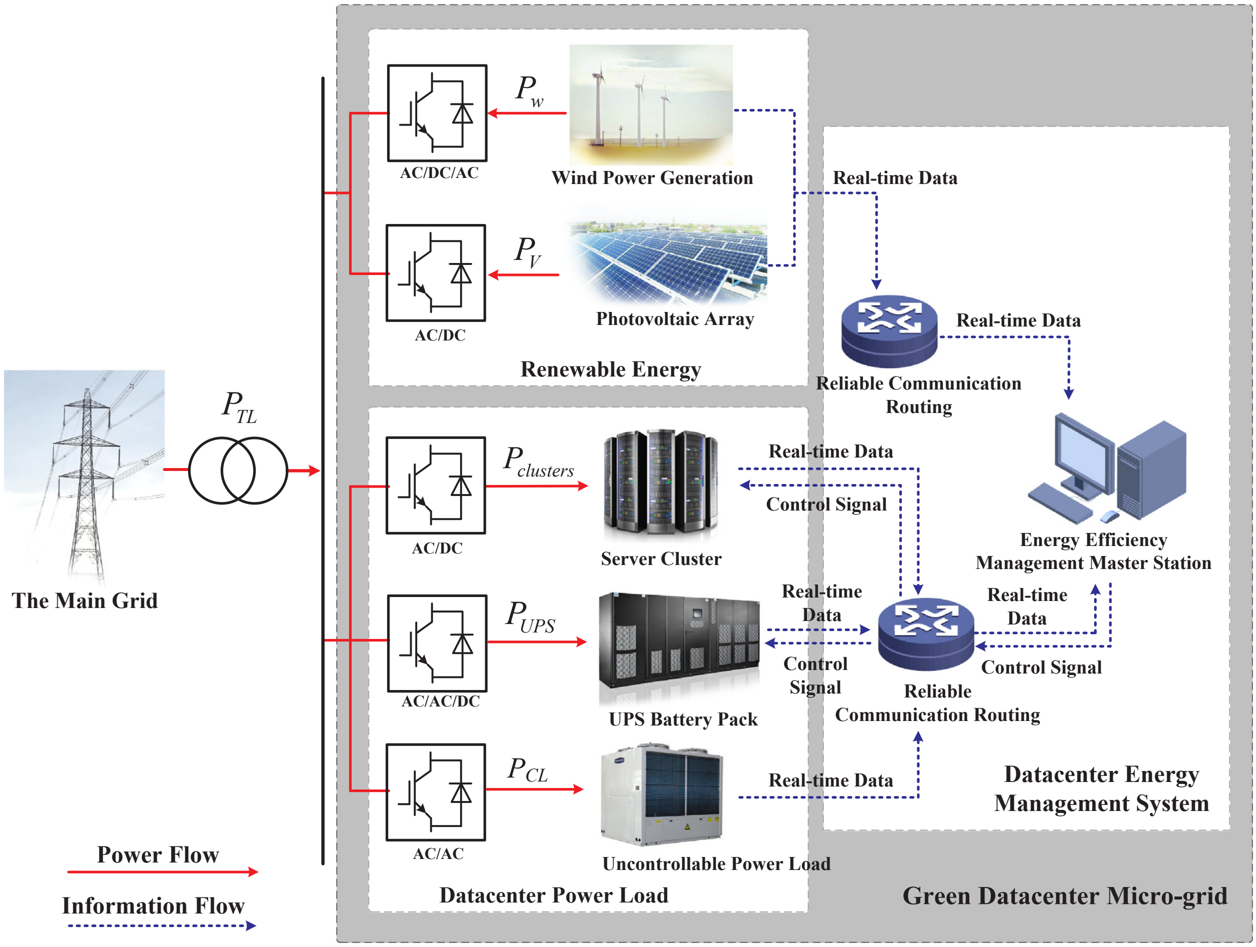

Fig. 3. Typical micro-grid framework of the renewable energy data center.

Table 1
The representation of symbolic in the Eq. (3).

Symbolic	Meaning
$P_{TL,i}$	The power of the utility power grids supplied for the intelligent park data center by the tie-line in minutes i
$P_{UPS,i}$	The real-time UPS battery power in minutes i. In this paper we assume that the value of discharging power is positive and charging power is negative
$P_{RE,i}$	The real time output power of renewable energy in minutes i. $P_{RE,i}$ can be generated from wind power or photovoltaic power, and so on
$P_{clusters,i}$	The power consumed by the server clusters in data center in minutes i
$P_{CL,i}$	The power consumed by data centers' cooling and lighting infrastructures, etc., in minutes i

server cluster power consumption $P_{Clusters,i}$ can be represented as:

$$P_{Clusters,i} = [P_{idle} + (P_{\max} - P_{idle})\cdot\eta_i]\cdot M_i \tag{6}$$

where M_i represents the number of active servers in minutes i. Because the frequent switching on and off of servers will increase energy consumption and severely reduce IT facility life, in this paper we do not employ the strategies of dynamically adjusting the number of active servers, i.e., $M_i = M_0$, which is the total number of servers in the data center. Only the resource utilization η_i is adjusted to realize the server cluster load controllability.

The average resource utilization η_i can be calculated as follow:

$$\eta_i = \frac{T_{busy,i}}{\Delta T_i} = \frac{[(\lambda_i + im_i - em_i)\cdot q]/(\delta\cdot M_0)}{q\cdot\Delta T_i} \tag{7}$$

where $T_{busy,i}$ is the server cluster busy time, and ΔT_i is the control step size, setting $\Delta T_1 = \Delta T_2 = \cdots = \Delta T_i = 1$ min in this paper. δ is the maximum processing capability of the signal server, i.e. the maximum number of processed basic tasks per minute. We further split ΔT to q even pieces. Because each piece is small enough, it can be safely assumed that each task arrives at the beginning of each piece. The initial average number of tasks in each ΔT_i is λ_i. Due to the fact that delay-tolerant tasks can be time shifted, the following should be considered when calculating the actual number of tasks in the ith minute: (1) im_i: the number of tasks migrating from its arriving time to time i; (2) em_i: the number of tasks migrating from minute i to the consecutive periods. Therefore, $\lambda_i' = \lambda_i + im_i - em_i$ is the actual number of processing tasks in the interval ΔT_i.

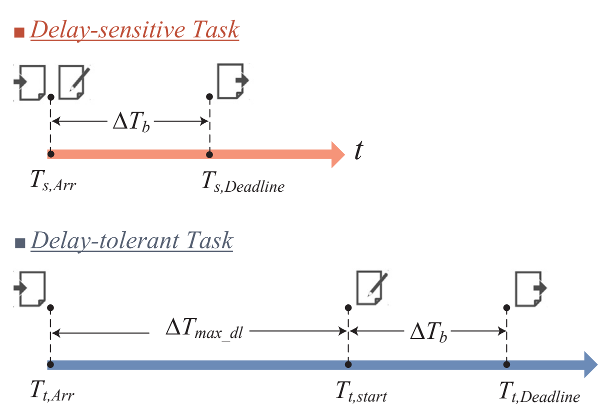

Fig. 4. Task processed or delay diagram.

Eqs. (5) and (6) represent the relationship between the data center's computing workload and power consumption. The model clearly reveals that the data center's power consumption can be precisely controlled by scheduling the processing tasks in each time slot ΔT_i. Therefore, based on the proposed time shift mechanism of delay-tolerant tasks, the server cluster workload scheduling model is established to realize the data center computing load's participation in demand response.

3.3. The UPS energy storage model

In order to guarantee the power supply reliability, data centers are often allocated a large number of UPS units, which realizes the uninterruptibility of power supply. One UPS unit constitutes the following two components: the bi-directional converters and batteries. The remaining power of battery can be measured by the state of charge. This paper employs the classic KiBaM (Kinetic Battery Model) [43] to formulate the UPS operation, and then proposes the UPS energy storage model:

$$P_{\mathrm{UPS},i} = \begin{cases} [\varphi\cdot(SOC_{i+1} - SOC_i)]\cdot\psi_{\mathrm{d}}, & \text{battery - charging} \\ [\varphi\cdot(SOC_{i+1} - SOC_i)]/\psi_{\mathrm{c}}, & \text{battery - discharging} \end{cases} \tag{8}$$

where SOC_i is the UPS battery's state of charge (SOC) in minutes i, which is the ratio of the battery's remaining electric quantity to the battery's capacity. ψ_c and ψ_d are the charging coefficient and discharging coefficient, respectively. φ is the power factor of UPS, which can be calculated by Eq. (9).

$$\varphi = \frac{N_s N_n V_{\mathrm{rated}} Q_{\mathrm{ups}}}{\Delta T_B} \tag{9}$$

where N_s and N_n are the number of the string batteries and parallel batteries, respectively. V_{rated} is the rated voltage of each battery. Q_{UPS} is the capacity of a single UPS battery (A·h), and $\Delta T_B = 1\mathrm{s}$.

Base on the proposed UPS energy storage model, we can adjust the state of UPS battery groups dynamically by charging or discharging power in a timely manner. This allows the UPS energy storage units to participate in the data center demand response in the premise of ensuring power supply reliability.

4. The tie-line power fluctuation smoothing algorithm based on data center holistic demand response

With the server cluster workload scheduling model and UPS energy storage model established in section III, the data center has the capability to participate in demand response. With the fine time granularity and flexible workload scheduling, the high frequency fluctuation of tie-line power can be easily smoothed, and low frequency large scale fluctuation can be reshaped by abundant UPS energy storage. This section presents this two-stage control strategy to realize the data center demand response.

4.1. Demand response control signals

Two-stage low-pass filters are used to obtain the demand response control signals. The initial tie-line power wave $P^0{}_{TL,i}$, which is the system input, is transferred through the two-stage low-pass filters, and the high-frequency control signal $P^1{}_{TL,i}$ and the low-frequency ones $P^*{}_{TL,i}$ are obtained. In the algorithm, the classical Butterworth low-pass filter is employed to reduce the system complexity. The time constants of two low-pass filters are T_1 and T_2, respectively. Fig. 5 shows the signal flow diagram, and the two stage control signals $P^1{}_{TL,i}$ and $P^*{}_{TL,i}$ can be calculated as follows:

$$\begin{cases} P^1_{TL,i} = \frac{\Delta T}{T_1}(P^0_{TL,i} - P^1_{TL,i-1}) + P^1_{TL,i-1} \\ P^*_{TL,i} = \frac{\Delta T}{T_2}(P^1_{TL,i} - P^*_{TL,i-1}) + P^*_{TL,i-1} \end{cases} \tag{10}$$

Given the first stage control signal $P^1{}_{TL,i}$, the regulated power quantity by server clusters is $\Delta P^1{}_{TL,i} = P^1{}_{TL,i} + P^0{}_{TL,i}$. Combining this with Eq. (3), the target power consumption of server cluster $P^*{}_{cluster,i}$ is calculated as:

$$P^*_{clusters,i} = P^0_{TL,i} + \Delta P^1_{TL,i} + (P_{W,i} + P_{V,i}) - P_{UL,i} \tag{11}$$

Similarly, in the second stage, the regulated quantity by the USP battery groups is $\Delta P^2{}_{TL,i} = P^*_{TL,i} - P^1{}_{TL,i}$. The target power consumption of UPS $P^*{}_{UPS,i}$ can be calculated as:

$$P^*_{UPS,i} = \Delta P^2_{TL,i} = P^*_{TL,i} - P^1_{TL,i} \tag{12}$$

4.2. Computing load time domain migration algorithm for servers' demand response

Ensuring the computing Service-Level Agreement (SLA), the server clusters demand response algorithm is operated to reach the control signal $P^*{}_{cluster,i}$ with dynamic time domain migration of the delay-tolerant tasks. This is a new type of migration based on time domain, called "*time-shift*", which is different from the traditional space migration of virtual machines among servers. The detailed control steps are listed as follows:

(1) Assume n types of new tasks reaching in minute i, in which there are m types of delay-sensitive tasks (numbered from 1 to m) and n-m types of delay-tolerant tasks (numbered from $m+1$ to n). Because only delay-tolerant tasks can be time shifted, the maximum delay time $t^{\max}_{delay,k,i}$ of task k is:

$$t^{\max}_{delay,k,i} = \begin{cases} 0 & k = 1, 2, \ldots, m \\ \lfloor \Delta T_{max\_dl} \rfloor_{k,i}\cdot\Delta T_i & k = m+1, \ldots, n \end{cases} \tag{13}$$

where $\lfloor\cdot\rfloor$ is the round down operation, which can ensure that the SLA is not violated.

(2) Based on the maximum delay time $t^{\max}_{delay,k,i}$ and the tie-line power control signal $P^*{}_{cluster,i}$, the delay-tolerant tasks can be precisely scheduled to satisfy the demand response. The optimization problem of server clusters' demand response can be modeled as:

$$\begin{aligned} \min \quad & \textstyle\sum_{i=1}^{T} (P_{clusters,i} - P^*_{clusters,i})^2 \\ s.\ t. \quad & \frac{\sum_{k=1}^{n}(\lambda_i + im_i - em_i)}{\delta\cdot M_0} \leqslant \Delta T_b \\ & 0 \leqslant em_i \leqslant \lambda_i \end{aligned} \tag{14}$$

The objective function is to make the actual tie-line power wave $P^*{}_{cluster,i}$ match the power control signal $P^*{}_{cluster,i}$, i.e., the difference between the two power waves is minimized. The first constraint guarantees that the delay operations do not violate the user's SLA requirements; and the second constraint shows that the parameter em_i is bounded, i.e., the number of backwards migrated tasks in minute i cannot be more than the total number of tasks.

While this optimization problem is solved, the delay-tolerant tasks can be scheduled with the optimization results. Then the high frequency fluctuation of the tie-line power can be well smoothed.

4.3. The regulation strategy of UPS battery storage

As the optimal control process of server clusters' demand response, when UPS battery groups receive the control signal $P^*{}_{UPS,i}$, each battery can adjust the working state, i.e., the charging or discharging power in real time, and then realize the tracking of target power curve. The objective function and constraints are presented in Eq. (15):

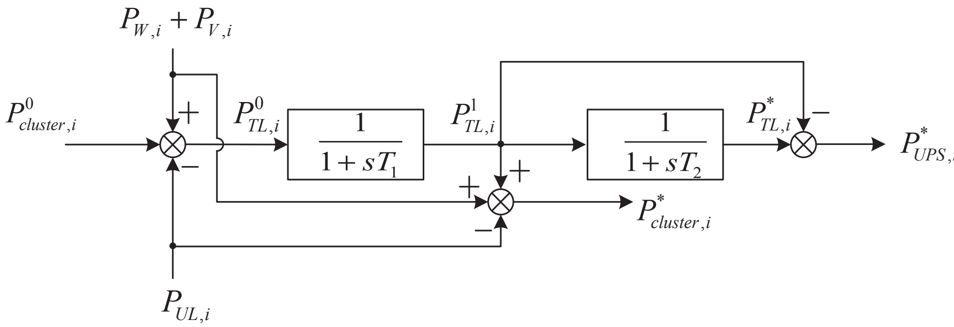

Fig. 5. Two-stage low-pass filters in the tie-line power smoothing algorithm.

$$\begin{aligned} \min \quad & \sum_{i=1}^{T}(P_{UPS,i}-P^*_{UPS,i})^2 \\ s.\,t. \quad & SOC_{\min} \leqslant SOC_i \leqslant SOC_{\max} \\ & \sum_{i=1}^{T} X_i \leqslant N^{swich}_{\max} \end{aligned} \tag{15}$$

where X_i is the marker of battery groups' charging or discharging times, $X_i = \begin{cases} 1, & (P_{UPS,i} \cdot P_{UPS,i-1}) < 0 \\ 0, & (P_{UPS,i} \cdot P_{UPS,i-1}) > 0 \end{cases}$. If, in the two adjacent time slots, $(P_{UPS,i} \cdot P_{UPS,i-1}) < 0$, $X_i = 1$ means there is one time of charge and discharge conversion. Otherwise, $X_i = 0$ means the battery is continuously charging or discharging in this two adjacent time slots.

In Eq. (15), the first constraint is the UPS battery's SOC constraint, which avoids the overcharging or discharging that may destroy the battery. In the second constraint N^{switch}_{max} is the maximum number of charging and discharging times allowed in the total control period, which can be set based on the UPS battery groups' operating requirements, because an unreasonable frequency of charging or discharging would accelerate the battery's aging and quickly wear it out [23], This would result in skyrocketing capital expenses and further increase the environmental burden (i.e. recycling problem) and the downtime for maintenance. In our demand response algorithm, we set N^{switch}_{max} to prevent this type of inappropriate operation.

Both Eqs. (14) and (15) are multi-variable nonlinear optimization problems. The variable of the first one is the number of time shift task units, and the variable of the second one is the batteries' SOC. We use the Generalized Reduced Gradient Method (GRG Algorithm) to solve these two typical nonlinear optimization problems [44], and obtain the optimal control scheme of data center's demand response.

5. Experiments, results and algorithm performance evaluation analysis

To evaluate the proposed algorithm's performance, we established a composite power supply system to the data center micro-grid, which includes wind power and photovoltaic power as renewable energy sources, UPS battery groups as energy storage units, and a micro-grid connection with utility power grids that includes some parameters that come from real distributed generation system.

5.1. Experiment settings and parameters

Hardware and software. We evaluate our proposed algorithm using a 30000-node server cluster, where each node consumes about 0.14 kW functioning at idle operation state, and 0.2 kW at max operation state. The server operation state has close relation with server resource utilization. The proposed algorithm runs on an additional server named Energy Management Master Station. With an accurate multimeter, we can measure the real-time power in our experiments. Furthermore, we assume 50% of the basic task units included in the experiments are delay-tolerant. It takes 0.1 min for a single server to process a basic task unit at full computing payloads.

Solar panel array. The experimental solar panel array model was established based on Tianjin Avenue Photovoltaic Power Generation Project, a subproject of the eco-city, which is capable of producing 3.3 MW of power (after DC to AC conversion). The real system is located in Tianjin Binhai New Area (40 km from the center of Tianjin), which is a cooperation project in Sino-Singapore Eco-City establised by China and Singapore [45]. Taking into consideration of the maximum load of the experimental intelligent park micro-grid, we scale the project's AC power production down to 2174 solar panels with a capacity of 500 kW of power. To carry out our experiment, we picked out one day data of solar energy output indicating that the solar panel array generates power from 7:00 am to 17:00 pm and reaches the maximum output power at around 13:00 pm.

Wind turbine. In our experiments, Shajingzi wind farm of Tianjin is employed [46], which can produce 200 MW of power. Using a similar method to the above solar panel array model, we estimated the production of a smaller wind farm installation. Taking the penetration of distributed renewable energy (set as 16%, 24% and 32% in this paper) into consideration, we scale the production of Shajingzi wind farm down to 800 kW of power (corresponding to the power of solar panel array mentioned above). To obtain the real-time wind power, we chose the same day data for the photovoltaic power output data and accurately forecasted wind power according to weather conditions.

Utility power grid. The reliability of the data center's power supply should be ensured by the power grid. When the renewable energy is not available, the main grid power is assumed to have sufficient capacity to maintain the data center's normal operation alone. In the experimental scenario, the intelligent park is connected to a utility power grid with a 35 kV substation. Traditionally, to reduce brown-energy costs and electricity bill, the data center firstly consumes supplied power of renewable energy (solar and wind). When renewable energy is unable to cover the data center's total energy consumption, the power of the main grid is supposed to compensate for the rest. However, we propose that this rule could be broken in order to ensure that the tie-line power is smooth.

The detailed experimental parameters, including UPS units and filter setting, are shown in Table 2.

In the following evaluated experiments, we performed one basic scenario experiment and a series of variable parameters' experiments, including different penetration of distributed renewable energy and different server cluster average resource utilization ranges. Each result is the average result of at least 100 independent experiments for the elimination of instability from the experimental distribution function.

5.2. Experiments in the basic scenario

In the basic experiment's scenario, the wind power and photovoltaic power output curves are shown in Fig. 6. The penetration of distributed renewable energy is set at 16%. The definition of the renewable energy penetration is described in Eq. (16) [47].

Table 2
Settings of experiment parameters.

	Parameter	Value
Server cluster	Number of servers M_0	30,000
	Idle power of single server P_{idle} (kW)	0.14
	Max power of single server P_{max} (kW)	0.2
	Proportion of delay-tolerant tasks (%)	50
	Service rate of single server, δ	10
Renewable energy	Number of solar panel	2174
	Total capacity of photovoltaic power (kW)	500
	Total capacity of wind power (kW)	800
UPS units	Number of batteries in series N_n	100
	Number of batteries in parallel N_s	300
	Rated voltage V_{rated} (V)	6
	Single battery capacity Q_{ups} (A·h)	100
	Charging coefficient of battery Ψ_c	0.95
	Discharging coefficient of battery Ψ_d	1.05
	Initial SOC S_0	0.75
	Lower limit of SOC S_{min}	0.5
	Upper limit of SOC S_{max}	1
	Max charging and discharging times $Switch_{max}$	50
Filter setting	The first time constant T_1 (min)	20
	The second time constant T_2 (min)	120
Simulation time	Simulation step ΔT (min)	1
	Total simulation time T_d (min)	1440

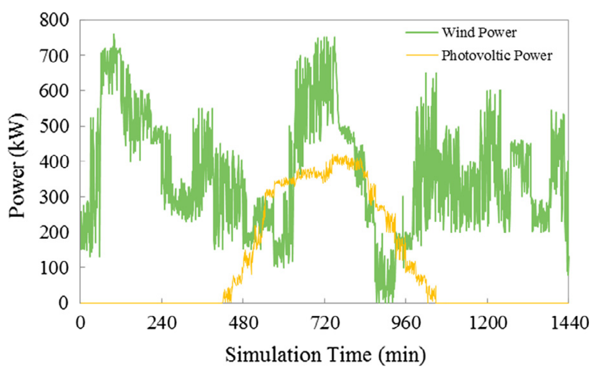

Fig. 6. The output of renewable energy.

$$P_m = \frac{\sum_{Renewable\ Eng} P_{cp}}{\max_{t=[0,T]}\{S_{load}(t)\}} \tag{16}$$

where P_{cp} is the installed power capacity of one kind of renewable energy, and the numerator is expressed as the total installed power capacity of renewable energy sources. S_{load} is the power consumer's apparent power, and the denominator is the peak apparent power in the whole cycle.

The initial data center utilization rate is from 30% to 50%, as shown in Fig. 7, and the adjustable range is set to [0.2, 0.8], i.e., η_{min} = 20%, η_{max} = 80%.

The major power consumer in the intelligent industrial park is the server clusters of data center for dealing with the stochastic incoming workloads. The initial tie-line power fluctuation in the intelligent park that has not been controlled by any demand response strategy is shown as the blue[1] curve in Fig. 8. It is obvious that due to the instability of the renewable energy output and the stochastic incoming computing workloads, the initial tie-line power shows great volatility and has many spikes.

Using the demand response tie-line power fluctuation smoothing algorithm proposed in this paper, the control signal of the server cluster

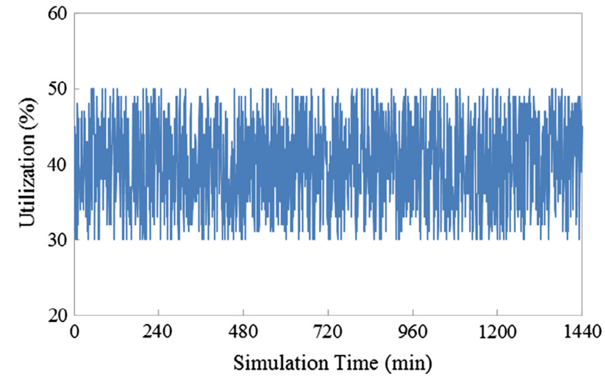

Fig. 7. Server cluster initial resource utilization.

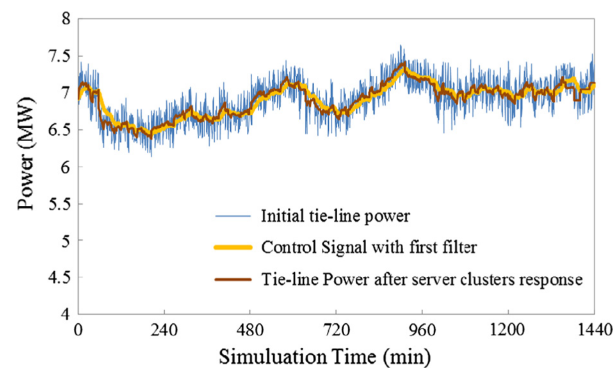

Fig. 8. Tie-line power change process.

can be obtained from the primary filter, shown as the yellow curve in Fig. 8. Because the algorithm dynamically adjusts computing workload in different time intervals in server clusters, the high-frequency power fluctuation in the tie-line is eliminated. In Fig. 8, the red curve is smoother than the blue one, and it also follows the target yellow curve closely.

Using the secondary filter to deal with the tie-line power red curve, the secondary control signal for the UPS battery groups' control can be obtained, shown as the yellow curve in Fig. 9. Following the control signal, the UPS battery groups are dynamically charged and discharged to compensate for the low-frequency power fluctuations in the micro-grid tie-line. The final results of the tie-line power with the server cluster and the UPS battery group responding together is shown as the red curve in Fig. 9. It can be easily seen that, in the condition of keeping the normal serviceability, data center micro-grid tie-line power fluctuations can be effectively regulated with the demand response strategy. In Fig. 9, the standard deviation of the tie-line power curves is reduced from 0.286 MW (blue curve) to 0.154 MW (red curve).

The rate of change ΔP_{TL} is also employed to evaluate the tie-line power smoothing effect by the demand response strategy as shown in the following equation:

$$\Delta P_{TL,i} = \frac{dP_{TL,i}}{dt} = \frac{P_{TL,i+1} - P_{TL,i}}{\Delta T} \tag{17}$$

The probability distribution of ΔP_{TL} is calculated and shown in Fig. 10. It is clear that with the demand response algorithm the tie-line power curve has obviously become smooth.

5.3. Evaluation of the adaptability of the demand response algorithm

The experiments with different scenarios are implemented to evaluate the adaptability of the proposed demand response algorithm in this section.

[1] For interpretation of color in Figs. 8 and 9, the reader is referred to the web version of this article.

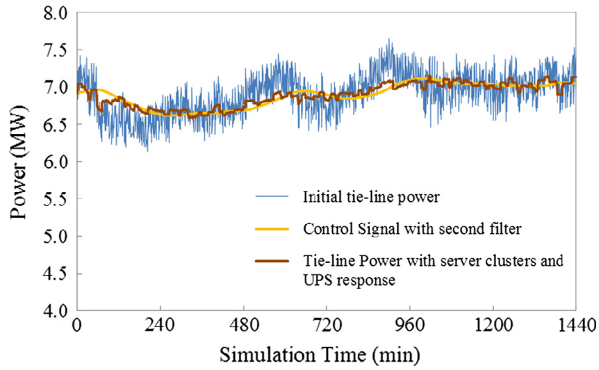

Fig. 9. Tie-line power fluctuation regulation result.

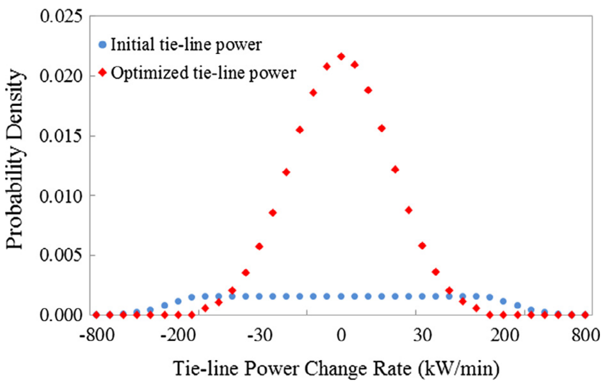

Fig. 10. Distribution of tie-line power fluctuation probability.

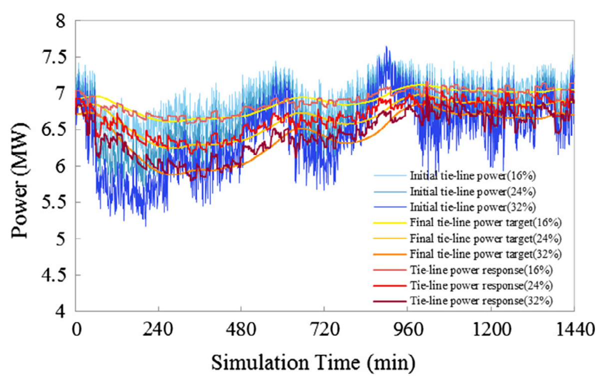

Fig. 11. Tie-line power change process with different renewable energy penetration.

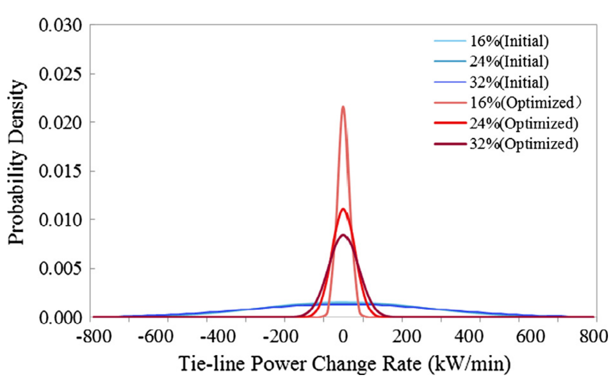

Fig. 12. Distribution of power fluctuation probability of tie-line with different renewable energy penetration.

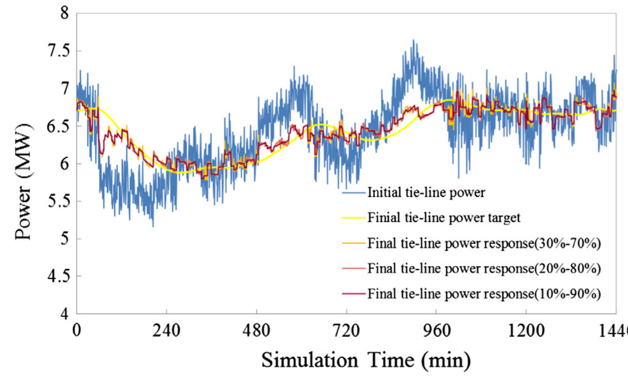

(a) Tie-line power change process (Final response)

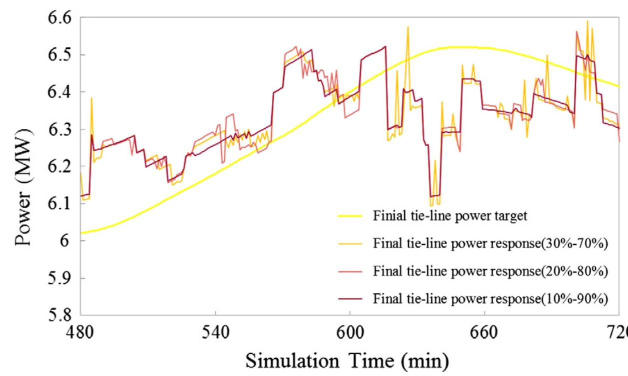

(b) Partial enlargement of tie-line power change process (Final response).

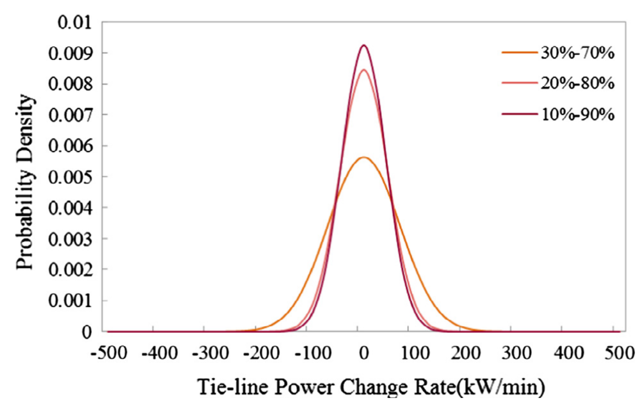

(c) Distribution of tie-line power fluctuation probability

Fig. 13. Tie-line power fluctuation stabilization comparison (Change in utilization range).

(1) *Experimental Scenarios with Different Renewable Energy Penetration*

Two contrastive experiments with 24% and 32% penetration are implemented to evaluate the algorithm performance in large-scale penetration of distributed renewable resources scenarios. The initial tie-line power curves and the results from the smoothing process using the demand response algorithm are shown in Fig. 11. With the increase of renewable energy permeability, it brings serious problems of intermittent energy supply to data center micro-grid. Using the proposed demand response algorithm, the severe fluctuate is smoothed even in the 32% penetration scenarios. The probability distribution curves of tie-line power fluctuations are shown in Fig. 12.

(2) *Experimental Scenarios with Different Server Cluster Average Resource*

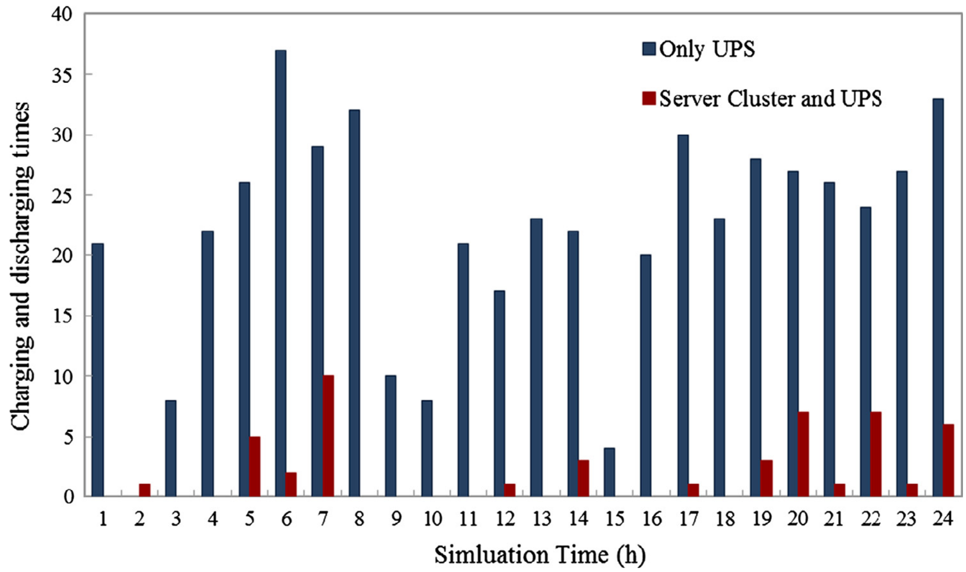

Fig. 14. UPS battery group charging and discharging statistics.

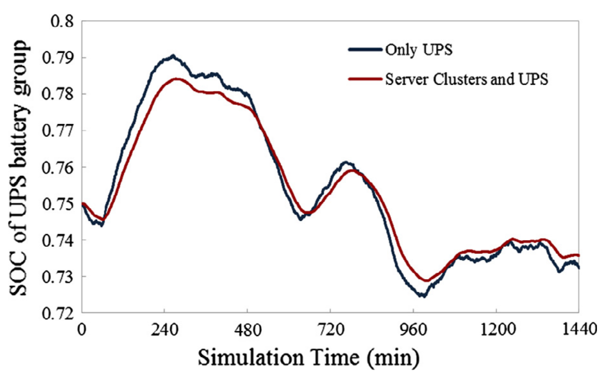

Fig. 15. UPS Battery group operating status.

Utilization Ranges

Because higher renewable energy penetration brings greater challenges to smooth tie-line power fluctuation, as shown in the experiment's result in the last section, we use the 32% penetration scenarios to evaluate the demand response algorithm with different ranges of server cluster average resource utilization.

In the experiments, three types of average CPU resource utilization ranges were set: [10%, 90%], [20%, 80%], [30%, 70%] and the smoothed tie-line power fluctuation curves are shown in Fig. 13. The figure shows that, under any set CPU resource utilization range, the proposed demand response algorithm can effectively follow the target control signal curve (the yellow curve in Fig. 13). In order to show the difference among experimental results, we added a partial enlargement graph shown in Fig. 13(b) and calculated the probability distribution of each tie-line power curve's change rate in Fig. 13(c). It can be seen clearly that, with widening server cluster resource utilization range, the stronger controllability of server clusters can smooth high frequency power fluctuations.

5.4. SOC of UPS battery group

A UPS unit with a great many battery groups is very important for a data center for providing backup power support, but it has a short life cycle as a result of frequent charging and discharging, which results in skyrocketing capital expenses and operating costs in the data center.

When the server scheduling participates in the demand response, it not only smoothes the high frequency power fluctuations, but can also reduce the UPS charging and discharging frequency. Fig. 14 shows the charging and discharging times as a function of time. It is clear that with the server clusters participating in the demand response, the battery's charging and discharging times are reduced significantly, which is greatly beneficial in extending the lifetime of UPS units. Therefore, establishing the IT load demand response controllable model and making the server clusters participate in demand response not only can smooth high frequency power fluctuations, but also reduce the capital expenses and operating costs for data center operator. The smoothing effect of UPS's SOC curves is presented in Fig. 15.

6. Conclusion

The intelligent industrial park powered by renewable energy has provided an effective way to realize sustainable development. However, the intermittency and instability of clean energy is a major concern. Considering the stability of energy supply for precision IT facility, this paper proposes a holistic demand response control algorithm to smooth the tie-line power fluctuations of data center with high density IT equipment. Based on the characteristics of data processing requirements and the infrastructure of power supply units in data center, the workload scheduling model and the UPS energy storage model are proposed to innovatively involve data centers in demand response. On the premise of computing service quality assurance and backup power reliability, the proposed novel algorithm successfully schedules the delay-tolerant tasks and controls the UPS battery groups' SOC to smooth the data center tie-line power fluctuations.

Extensive experimental results show that (1) with the two-stage low-pass filters, data center micro-grid tie-line power fluctuations can be effectively regulated, in which the high-frequency power fluctuation is eliminated by computing workload time-shift control and the low-frequency ones is smoothened by UPS battery group dynamical management. (Section 5.2); (2) the proposed algorithm has good adaptability in different renewable energy penetration scenarios (Part 1, Section 5.3) and with different server cluster computing load (Part 2, Section 5.3); (3) the SOC control strategy used in our proposed algorithm has significantly reduced the frequency of UPS battery's charging and discharging conversion, which is beneficial in protecting the UPS and reducing the capital expenses for data center operator (Section 5.4).

Based on the model and prototype built and tested in our data center, we will enhance our approach to be applied to a real-life intelligent industrial park with large-scale data center and fine tune its performance in the future.

Acknowledgments

This paper is supported by the National Key Research and Development Program of China (2017YFB0903000); National Natural Science Foundation of China (61571324); Natural Science Foundation of Tianjin (16JCZDJC30900); and National Program of International S&T Cooperation (2013DFA11040).

References

[1] Sun D-W, Chang G-R, Chen D, Xing-Wei W. Profiling, quantifying, modeling and evaluating green service level objectives in cloud computing environments. Chinese J Comput 2013;36(7):1509–29.
[2] Drozdowski M, Marsza J. Time and energy performance of parallel systems with hierarchical memory. J Grid Comput 2016;14(1):153–70.
[3] Mohsenian-Rad AH, Leon-Garcia A. Coordination of cloud computing and smart power grids. Smart grid communications (SmartGridComm). First IEEE international conference on. 2010. p. 368–72.
[4] Zhou Z, Liu F, Zou R, Liu J, Xu H, Jin H. Carbon-aware online control of geo-distributed cloud services. IEEE Trans Parallel Distrib Syst 2016;27(9):2506–19.
[5] Quan H, Srinivasan D, Khambadkone AM, et al. A computational framework for uncertainty integration in stochastic unit commitment with intermittent renewable energy sources. Appl Energy 2015;152:71–82.
[6] Li Z, Qiu F, Wang J. Data-driven real-time power dispatch for maximizing variable renewable generation. Appl Energy 2016;170(1):304–13.
[7] Islam MA, Ren S, Mahmud AH, Quan G. Online energy budgeting for cost minimization in virtualized data center. IEEE Trans Serv Comput 2016;9(3):421–32.
[8] Vithayasrichareon P, Riesz J, Macgill I. Operational fl exibility of future generation portfolios with high renewables. Appl Energy 2017;206(8):32–41.
[9] Amini MH, Nabi B, Haghifam M-R. Load management using multi-agent systems in smart distribution network. IEEE, 2013. 2013. p. 1–5.
[10] Nguyen N, Member S, Mitra J, Member S. An analysis of the effects and dependency of wind power penetration on system frequency regulation. IEEE Trans Sustain Energy 2016;7(1):354–63.
[11] Deng X, Wu D, Shen J, He J. Eco-aware online power management and load scheduling for green cloud datacenters. IEEE Syst J 2016;10(1):78–87.
[12] Fairley P. Blockchain world-Feeding the blockchain beast if bitcoin ever does go mainstream, the electricity needed to sustain it will be enormous. IEEE Spectr 2017;54(10):36–59.
[13] Lee J, Vegas L. An analysis of energy and hardware impacts on the bitcoin mining network. ACM Trans Econ Comput 2015;1(1):1–20.
[14] Liu L, Sun H, Li C, Hu Y, Xin J, Zheng N, et al. RE-UPS: an adaptive distributed energy storage system for dynamically managing solar energy in green datacenters. J Supercomput 2016;72(1):295–316.
[15] Ghamkhari M, Mohsenian-rad H. Energy and performance management of green data centers: a profit maximization approach. IEEE Trans Smart Grid 2013;4(2):1017–25.
[16] Guo Y, Gong Y, Fang Y, Khargonekar PP, Geng X. Energy and network aware workload management for sustainable data centers with thermal storage. IEEE Trans Parallel Distrib Syst 2014;25(8):2030–42.
[17] Li C, Qouneh A, Li T. iSwitch: coordinating and optimizing renewable energy powered server clusters. In: Computer architecture (ISCA), 2012 39th annual international symposium on, vol. 00; 2012. p. 512–23.
[18] Aksanli B, Venkatesh J, Zhang L, Rosing T. Utilizing green energy prediction to schedule mixed batch and service jobs in data centers. ACM SIGOPS Oper Syst Rev 2011;455(3):53–7.
[19] Sharma N, Sharma P, Irwin D, Shenoy P. Predicting solar generation from weather forecasts using machine learning. Smart grid communications (SmartGridComm). IEEE international conference on. 2011. p. 528–33.
[20] Li C, Zhou R, Li T. Enabling distributed generation powered sustainable high-performance data center. In: High performance computer architecture (HPCA2013). 2013 IEEE 19th international symposium on; 2013. p. 35–46.
[21] Apple and the Environment. <https://www.apple.com/environment/> [cite on Dec. 2016].
[22] Data Center Knowledge. <http://www.datacenterknowledge.com/> [cite on Dec. 2017].
[23] eBay plans data center. <https://www.lvgea.org/ebay-plans-data-center-expansion-in-las-vegas/> [cite on Nov. 2016].
[24] Arlitt M, Bash C, Blagodurov S, Chen Y, Christian T, Gmach D, et al. Towards the design and operation of net-zero energy data centers. In: Thermal and thermomechanical phenomena in electronic systems (ITherm). 2012 13th IEEE intersociety conference on; 2012. p. 552–61.
[25] Ren C, Wang D, Urgaonkar B, Sivasubramaniam A. Carbon-aware energy capacity planning for datacenters. In: Modeling, analysis & simulation of computer and telecommunication systems (MASCOTS). 2012 IEEE 20th international symposium on; 2012. p. 391–400.
[26] Xia Y, Zhou M, Luo X, Pang S, Zhu Q. A stochastic approach to analysis of energy-aware DVS-enabled cloud datacenters. IEEE Trans Syst Man Cybern Syst 2015;45(1):73–83.
[27] Cho J, Kim Y. Improving energy efficiency of dedicated cooling system and its contribution towards meeting an energy-optimized data center. Appl Energy 2016;165(1):967–82.
[28] Adefarati T, Bansal RC. Reliability and economic assessment of a microgrid power system with the integration of renewable energy resources. Appl Energy 2017;206(8):911–33.
[29] Shi J, Xue F, Ling L, Li X, Qin Z, Li Y, et al. Combining model-based and heuristic techniques for fast tracking the global maximum power point of a photovoltaic string. J Power Electron 2017;17(2):476–89.
[30] Zhang F, Maddy J, Premier G, Guwy A. Novel current sensing photovoltaic maximum power point tracking based on sliding mode control strategy. Sol Energy 2015;118(8):80–6.
[31] Shi J, Ling L, Xue F, Qin Z, Li Y, Lai Z, et al. Combining incremental conductance and firefly algorithm for tracking the global MPP of PV arrays. J Renew Sustain Energy 2017;9(2):023501.
[32] Patel MR. Wind and solar power systems. CRC Press; 2006.
[33] Kliazovich D, Bouvry P, Ullah S. DENS: data center energy-efficient network-aware scheduling. Cluster Comput 2013;16(1):65–75.
[34] Li T, Ren Y, Yu D, Jin S. RAMSYS: resource-aware asynchronous data transfer with multicore systems. IEEE Trans Parallel Distrib Syst 2017;28(5):1430–44.
[35] Christy Sujatha D, Abimannan S. Energy efficient free cooling system for data centers. In: Cloud computing technology and science (CloudCom). 2011 IEEE third international conference on; 2011. p. 646–51.
[36] Saddler H. South Australia makes a fresh power play in its bid to end the blackouts. Chain React 2017;129(4):14–5.
[37] Liu L, Sun H, Li C, Li T, Xin J, Zheng N. Managing battery aging for high energy availability in green datacenters. IEEE Trans Parallel Distrib Syst 2017;28(12):3521–36.
[38] Ghamkhari M, Wierman A, Mohsenian-Rad H. Energy portfolio optimization of data centers. IEEE Trans Smart Grid 2017;8(4):1898–910.
[39] Goiri Í, Le K, Nguyen TD, Guitart J, Torres J, Bianchini R. Greenhadoop_Leveraging green energy in data-processing frame-works. In: Proceedings of the 7th ACM European conference on computer systems; 2012. p. 57–70.
[40] Wang D, Liu X. A resource scheduling strategy for cloud computing platform of power system simulation based on dynamic migration of virtual machine. Autom Electr Power Syst 2015;39(12):97–105.
[41] Kumar S, Nadjaran A, Gopalaiyengar SK, Buyya R. SLA-based virtual machine management for heterogeneous workloads in a cloud datacenter. J Netw Comput Appl 2014;45(1):108–20.
[42] Xu L, Xu K, Jiang Y, Ren F, Wang H. Throughput optimization of TCP incast congestion control in large-scale datacenter networks. Comput Netw 2017;124(1):46–60.
[43] Manwell JF, McGowan JG. Lead acid battery storage model for hybrid energy systems. Sol. Energy 1993;50(5).
[44] Yang T. Optimization design. Tianjin, China: China Machine Press; 2014. p. 133–43.
[45] Sino-Singapore Tianjin eco-city. <http://www.tianjineco-city.com/> [cite on Jan. 2018].
[46] Shajingzi wind farm. <http://www.gov.cn/jrzg/2011-02/15/content_1803906.htm> [cite on Dec. 2017].
[47] Zhang Y, Guo L, Jia H, Li Z, Lu Z. An energy storage control method based on state of charge and variable filter time constant. Autom Electr Power Syst 2012;36(6):34–8.